Arch Biol Sci. 2016;68(4):853-861 DOI:10.2298/ABS151210075H

GLUCOSE-INDUCED LIPID DEPOSITION IN GOOSE PRIMARY HEPATOCYTES IS DEPENDENT ON THE PI3K-AKT-MTOR SIGNALING PATHWAY

Chunchun Han[1,*], Shouhai We[2], Fang He[1], Qi Song[1], Xiangping Xiong[1], Fengjiang Ye[1], Dandan Liu[1], Huofu Wan[1], Hehe Liu[1], Liang Li[1], Hongyong Xu[1], Feng Xu[1] and Xianyin Zeng[2]

[1] *Institute of Animal Breeding and Genetics, Sichuan Agricultural University*, Chengdu, Sichuan, 61130, P.R. China
[2] *College of Life Science, Sichuan Agricultural University*, Ya'an, Sichuan, 625014, P.R. China

***Corresponding author**: chunchunhai_510@163.com

Received: December 10, 2015; **Revised**: January 15, 2016; **Accepted**: January 16, 2016; **Published online**: August 19, 2016

Abstract: Previously we showed that fatty liver formation in overfed geese was accompanied by PI3K-Akt-mTOR pathway activation and changes in plasma glucose concentrations. Here, we show that glucose acts in goose hepatocellular lipid metabolism through the PI3K-Akt-mTOR signaling pathway. We observed that glucose increased lipogenesis, decreased fatty acid oxidation and increased very low density lipoprotein triglyceride (VLDL-TG) assembly and secretion. Co-treatment with glucose and inhibitors of the PI3K-Akt-mTOR pathway (LY294002, rapamycin, NVP-BEZ235) decreased the levels of factors involved in lipogenesis and increased the levels of factors involved in fatty acid oxidation and VLDL-TG assembly and secretion. These findings show that inhibition of the PI3K-Akt-mTOR pathway decreased glucose-induced lipogenesis, inhibited the downregulation of fatty acid oxidation by glucose and increased the upregulation of VLDL-TG assembly and secretion by glucose. The results presented herein provide further support for the role of the PI3K-Akt-mTOR pathway in lipid metabolism as we showed that in goose primary hepatocytes, glucose acts through the PI3K-Akt-mTOR-dependent pathway to stimulate lipid deposition by increasing lipogenesis and decreasing fatty acid oxidation and VLDL-TG assembly and secretion.

Key words: glucose; PI3K-Akt-mTOR pathway; lipogenesis; fatty acid oxidation; VLDL assembly and secretion

INTRODUCTION

Glucose is an important energy source for liver metabolism. Normal glucose transport and metabolism are among the key factors that maintain the normal physiological function of liver cells. Glucose can increase lipid droplets by inducing the expression of lipogenic genes [1] and decreasing mRNA expression levels of the genes involved in mitochondrial fatty acid oxidation [2]. The PI3K-Akt-mTOR (phosphatidylinositol-3 kinase/protein kinase-B/mammalian target of rapamycin) pathway has been linked to an extraordinarily diverse group of cellular functions via the regulation of cell proliferation [3], survival and intracellular trafficking [4]. The PI3K-Akt signal transduction pathway mediates lipogenesis in human kidney cells (HKC) treated with high glucose, and the blockade of the PI3K-Akt pathway prevents the activation of the fatty acid synthesis pathway through SREBP-1 and FAS expression [5]. The PI3K-Akt signaling pathways are activated in the glomeruli of diabetic rats and in mesangial cells cultured under high glucose concentrations [6,7]. Although some researchers have reported a relationship between lipogenesis and activation of the PI3K-Akt pathway [8,9], it is unclear whether the PI3K-Akt-mTOR pathway plays a role in glucose-induced lipid deposition.

Unlike human fatty liver, waterfowl liver can exhibit nonpathological hepatic steatosis, with the functional integrity of hepatocytes remaining intact. In our previous study, overfeeding was accompanied by lipid deposition in the liver, a change in blood glucose concentration [10] and activation of the PI3K-Akt-mTOR signaling pathway [11]. We speculated that the PI3K-Akt-mTOR pathway mediates glucose-induced lipid deposition. Therefore, in this study, goose primary hepatocytes were treated with glucose and inhibitors of the PI3K-Akt-mTOR pathway, alone or together, to detect changes in lipogenesis, fatty acid oxidation

and VLDL assembly and secretion to ascertain the role of the PI3K-Akt-mTOR pathway in glucose-induced lipid deposition.

MATERIALS AND METHODS

Primary hepatocyte isolation and culture

Hepatocytes were isolated from three 30-day-old Tianfu meat geese that were obtained from the Experimental Farm for Waterfowl Breeding at Sichuan Agricultural University, using a modification of the "two-step procedure" described by Seglen [12]. The culture medium is the same as that in our previous paper [8]. Cultures were incubated at 40°C in a humidified atmosphere containing 5% CO_2; the medium was renewed after 3 h, and after 24 h it was replaced with serum-free media. After an additional 24 h, the cells were separately treated with serum-free media supplemented with 0, 5 and 35 mmol/L of glucose and incubated for 24 h. The control cells were cultured with serum-free media for 24 h. Some cells were treated with serum-free media supplemented with PI3K-Akt-mTOR pathway inhibitors (20 μmol/L LY294002, 30 nmol/L rapamycin, and 1 μmol/L NVP-BEZ235, respectively) for 24 h, followed by the addition of 5 mmol/L glucose or 35 mmol/L glucose and incubation for an additional 24 h. The cell treatment is explained in Table 1. After the incubation, the culture media and cells were cooled on ice and collected. In each case, the experiments were repeated three times.

Table 1. Introduction of cell treatment.

Treatment	Glucose (mmol/L)	LY294002 (μmol/L)	Rapamycin (nmol/L)	NVP-BEZ235 (μmol/L)
1	0	0	0	0
2	0	20	0	0
3	0	0	30	0
4	0	0	0	1
5	5	0	0	0
6	5	20	0	0
7	5	0	30	0
8	5	0	0	1
9	35	0	0	0
10	35	0	0	0
11	35	20	0	0
12	35	0	30	0

Measurement of intracellular and extracellular TG concentrations

The culture media were collected for measuring extracellular TG concentrations. In order to measure intracellular TG concentrations, cell samples were collected and shaken for 1 h using an ultrasonic processor and then a 0.5-ml isovolumic mixture of chloroform and methanol (2/1, v/v) was directly added. The TG levels were quantified using a triglyceride GPO-POD assay kit (Biosinc, China) by a colorimetric method as described by Fossati et al. [13].

Measurement of extracellular VLDL concentration

The supernatant was obtained after the culture media samples were collected and centrifuged for 20 min at 1000×g. The extracellular VLDL concentration in the supernatant was measured using a chicken VLDL ELISA kit (GBD, USA). As described in the manufacturer's instructions for use, the microtiter plate provided in this kit had been precoated with an antibody specific to VLDL. After the enzyme-substrate reaction was terminated, the color change was measured spectrophotometrically at 450 nm. The concentration of VLDL in the samples was determined by comparing the optical density (OD) value of the samples to the standard curve.

Oil Red O staining

Hepatocytes were stained with Oil Red O to examine the amount of lipid accumulation in the cells. The hepatocytes (4×10^4 cells/well) were cultured on four-well culture slides, fixed in formalin, and stained [14]. The wells were fixed with Baker's formalin for 15 min, rinsed with distilled water, equilibrated in 100% propylene glycol for 2 min, and then stained with Oil Red O for 10 min; free Oil Red O was removed after 60% propylene glycol (vol/vol) was added to the wells for 1 min. The Oil Red O was extracted with the addition of isopropanol, and Oil Red O was determined in aliquots from wells after shaking the culture plates for 30 min at room temperature. Then, cells were examined by phase contrast microscopy at 200x magnification.

Oil Red O extraction

The steps for Oil Red O extraction were similar to those described above for Oil Red O staining using a method described previously [15]. After the cells were stained with 1% filtered Oil Red O, the Oil Red O solution was removed and the cells did not need to be washed. Intracellular triglyceride levels in the cells were agitatedly extracted with 100% isopropanol solution of 2 mL for 15 min in a shaker. Finally, a hole with DMSO was used to adjust zero, and the OD value of each hole was monitored by a spectrophotometer at 510 nm.

Measurement of the protein content in culture cells

The protein content was determined with ELISA kits according to the manufacturer's instructions (MyBioSource, Inc., USA). The microtiter plates provided in all kits were precoated with an antibody specific to the responding protein. The enzyme-substrate reaction was terminated by the addition of a sulfuric acid solution, and the absorbance at 450 nm was read using a plate reader. The protein content in the samples was calculated from polynomial second order or exponential standard curves obtained from the standards included in each assay.

Isolation of total RNA and real-time RT-PCR

Total RNA was isolated from cultured cells using TRIzol (Invitrogen, USA) and reverse-transcribed using the Primer Script TM RT system kit for real-time PCR (TaKaRa, Japan) according to the manufacturer's instructions. The quantitative real-time PCR was performed on the Cycler system (one cycle of 95°C for 10 s, followed by 40 cycles of 95°C for 5 s and 60°C for 40 s). An 80-cycle melt curve was performed, starting at 55°C and increasing by 0.5°C every 10 s, to determine primer specificity. Specific primers were designed according to the goose gene sequences listed in Table 2. PCR products were diluted 16-fold and used to generate the calibration curve and the amplification rate (R) for each gene. For each experimental sample, a normalized target gene level (Exp) corresponding to the target gene expression level relative to β-actin, 18S and UBC (housekeeping genes) expression levels, was determined by the $2^{-\Delta\Delta Ct}$ method as previously described [16]. The final results were calculated by extracting the cube root of the three relative mRNA expression levels of each gene relative to β-actin, 18S and UBC. The results for each individual were repeated three times and averaged.

Table 2. Primer sequences for real-time PCR.

Gene Name	Upstream (5′-3′)	Downstream (5′-3′)	Product size (bp)	Accession number
PI3K	ACCCAAGCGAGGATGAGG	TGTTGCCCGTGTTGAATG	241	KF011500
Akt1	TGCTGGATAAAGATGGAC	CTGGTTGTAGAAAGGGAG	215	KF011501
mTOR	TCATTTGTTACTACCTCCCA	TTTCTAGAGCAGCTTTGCGAGCCAC	93	KC424580
S6K	CTCAACTTGCCTCCCTAC	AACTTCTCCAGCATCTCC	111	KC424581
4EBP1	CCACCTTCTGACCTTCCG	CATTCGCTTTCTCATCGTAG	103	KF011497
Rptor	GAAAGGCAAATATCAACCG	CAGCCATCACAGACACCA	223	KF011498
Akt2	GCGATGCTCCATCACCTCC	CGCCTGCCCTTCTACAACC	183	KF857233
SREBP-1	CGAGTACATCCGCTTCCTGC	TGAGGGACTTGCTCTTCTGC	92	EU333990
FAS	TGGGAGTAACACTGATGGC	TCCAGGCTTGATACCACA	109	EU770327
ACCα	TGCCTCCGAGAACCCTAA	AAGACCACTGCCACTCCA	163	EF990142
PPARα	ATCTATCCCTGGCTTCTCCA	AGCATCCCATCCTTGTTCATT	117	AF481797
MTTP	CCCGATGAAGGAGAGGAA	AAAATGTAACTGGCCTGAGT	85	GO240734
FoxO1	CATCCCTTCAGTCTGGTCAA	GAAAGGCTGGGTAAAGTAG	265	GW342986
CPT1	GTCTCCAAGGCTCCGACAA	GAAGACCCGAATGAAAGTA	193	GW342945
ACOX1	ACAGAAAGAGCAAGGAGGAT	GCACGAGGTCAACAGAAGT	51	KC424582
apoB	CTCAAGCCAACGAAGAAG	AAGCAAGTCAAGGCAAAA	153	GW342984
PPARγ	CCTCCTTCCCCACCCTATT	CTTGTCCCCACACACACGA	108	AF481798.1
LXRα	CCCAGCCCTTCCCACAAACT	CTGCCTCGCTTCACGGTTATTAG	156	HM138512
ChREBP	AAGAAGCGGCTCCGAAAG	TGGTGGGTGCTGGGTGT	236	GW342987.1
β-actin	CAACGAGCGGTTCAGGTGT	TGGAGTTGAAGGTGGTCTCG	92	M26111.1
UBC	AGGGTGGATTCTTTCTGG	ACTGAGTTTGGAGGGAGC	243	GO240773.1
18S	TTGGTGGAGCGATTTGTC	ATCTCGGGTGGCTGAACG	129	L21170.1

Western blotting

Hepatocytes were washed twice and collected in ice-cold PBS. Total protein extracts were obtained using a reducing SDS buffer. Protein concentrations were determined on diluted samples using the Bradford procedure. Equal amounts of protein (100 μg) were separated by 6% SDS-PAGE and transferred to membranes. Membranes were blocked in a TBS solution with 5% nonfat dry milk and then incubated with rabbit against acetyl-CoA carboxylase-α (ACCα), ribosomal protein S6 kinase, 70 kDa, polypeptide 1 (S6K) or p-S6K antibodies (1:1000; Beijing Biosynthesis Biotechnology, China). Goat anti-rabbit horseradish peroxidase-conjugated IgG at 1:2000 (Beijing Biosynthesis Biotechnology, China) was used as the secondary antibody, and the signals were detected using an ECL Western blot detection kit (Beyotime Institute of Biotechnology, China). After analysis, the membranes were blotted with α-tubulin antibody at 1:1000 (Beijing Biosynthesis Biotechnology, China) to normalize for protein amount. The blot images were digitized with a luminescent image analyzer (LAS-1000, Fuji Photo Film).

Statistical analysis

All experimental data are presented as the means±SD. One-way ANOVA was used to assess the differences (Prism version 4.02; Graphpad Software Inc.) in the detected factors. If ANOVA revealed significant effects, post hoc tests were performed and means were compared by Tukey's test using the SAS 9.13 package (SAS Institute Inc, Cary, NC). $P<0.05$ was accepted as the level of significance. Every experiment was repeated with three biological samples, and each sample was run in triplicate.

RESULTS

Inhibition of the PI3K-Akt-mTOR signaling pathway inhibited the glucose-induced stimulation through this pathway

To verify the activation of the PI3K-Akt-mTOR signaling pathway by glucose, the collective effects of glucose and PI3K-Akt-mTOR signaling pathway inhibitors on the protein content and mRNA expression level of the PI3K-Akt-mTOR signaling pathway was assessed. As shown in Figs. 1a and 1b, compared with the control group 5 mmol/L glucose had no evident effect on the protein activities of PI3K, Akt, mTOR, 4EBP1 and S6K, while 35 mmol/L glucose significantly increased the activities of these proteins. After the combined treatment with glucose and LY294002, rapamycin or NVP-BEZ235, the activities of the tested proteins were lower than those after single glucose treatment. Western blotting (Fig. 1c) revealed that the combined treatment with 35 mmol/L glucose and LY294002, rapamycin or NVP-BEZ235 decreased the protein expression levels of S6K and p-S6K.

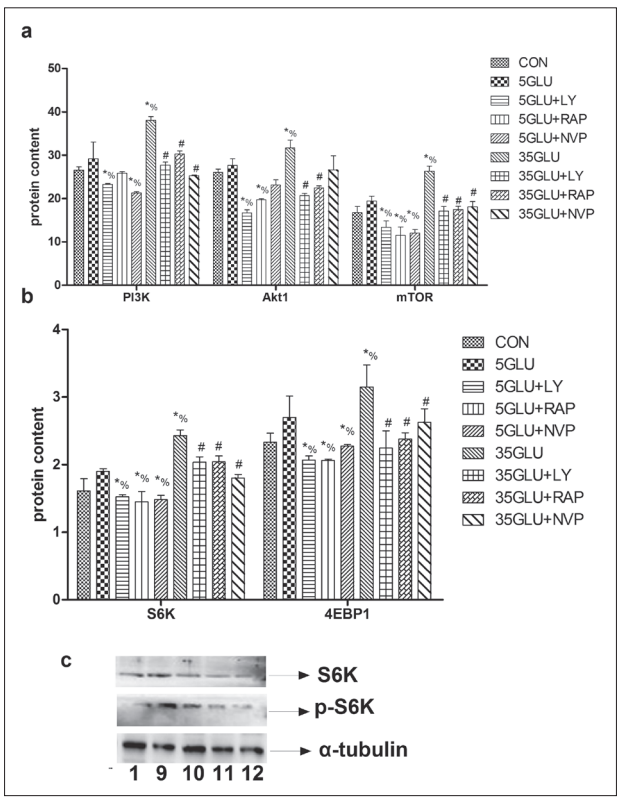

Fig. 1. Inhibitors of the PI3K-Akt-mTOR signaling pathway decreased the glucose-stimulated protein content of proteins in this pathway. **a** and **b** – protein contents of factors involved in the PI3K-Akt-mTOR pathway. The unit of PI3K is pmol/mL, the units of Akt1 and mTOR are pg/mL, and the units of S6K and 4EBP1 are ng/mL. **c** – Western blot of S6K and phosphorylated (p)-S6K. The symbols "CON, 5GLU, 35GLU, LY, RAP, NVP" in the right legend and under the blot indicate control, 5 mmol/L glucose, 35 mmol/L glucose, 20 μmol/L LY294002, 30 nmol/L rapamycin, and 1 μmol/L NVP-BEZ235, respectively. "*" above the bars indicates significant differences between all groups and the control group at $P<0.05$; "%" above the bars indicates significant differences between all groups and 5GLU at $P<0.05$; "#" above the bars indicates significant differences between all groups and 35GLU at $P<0.05$. Each blot is representative of three independent experiments.

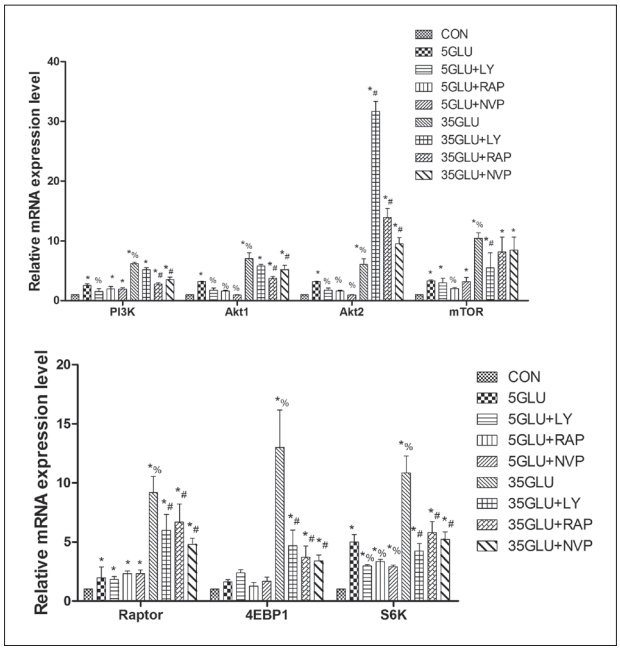

Fig. 2. PI3K-Akt-mTOR signaling pathway inhibitors decreased the stimulation of glucose on the relative mRNA expression levels of genes in this signal pathway. The symbols "CON, 5GLU, 35GLU, LY, RAP, NVP" in the right legend and under the blot indicate control, 5 mmol/L glucose, 35 mmol/L glucose, 20 μmol/L LY294002, 30 nmol/L rapamycin, and 1 μmol/L NVP-BEZ235, respectively. "*" above the bars indicates significant differences between all groups and the control group at P<0.05; "%" above the bars indicates significant differences between all groups and 5GLU at P<0.05; "#" above the bars indicates significant differences between all groups and 35GLU at P<0.05.

Fig. 2 shows that the inhibitors of the PI3K-Akt-mTOR signaling pathway decreased the glucose-promoted activation of the mRNA expression level of genes involved in the PI3K-Akt-mTOR pathway. Compared to the control group, glucose treatment increased the mRNA expression levels of PI3K, Akt1, Akt2, mTOR, regulatory associated protein of mTOR, complex 1 (Rptor), eukaryotic translation initiation factor 4E binding protein 1 (4EBP1) and S6K. Compared with 5 mmol/L glucose, 35 mmol/L glucose had a more pronounced effect on the mRNA expression levels of these genes. Compared with the glucose-only treatment, after the combined treatment with glucose and LY294002, rapamycin or NVP-BEZ235, the mRNA expression levels of all tested genes significantly decreased. These results confirmed that glucose stimulates PI3K-Akt-mTOR signaling pathways.

Inhibition of the PI3K-Akt-mTOR signaling pathway changed the effect of glucose on lipid metabolism

To test the hypothesis that the regulation of lipid accumulation by glucose is connected to the modulation of PI3K-Akt-mTOR signaling, the effect of glucose and the PI3K inhibitor LY294002, the mTOR inhibitor rapamycin, and the Akt-mTOR dual inhibitor NVP-BEZ235 on lipid accumulation was assessed. As shown in Figs. 3a-3e, 5 mmol/L glucose had no evident effect either on the intra- and extracellular concentrations of TG, the lipid content, the extracellular VLDL concentration, or on the protein content of fatty acid synthase (FAS), ACCα and CPT1. After treatment with 35 mmol/L glucose, the levels of these tested factors changed significantly. After co-treatment with glucose and LY294002, rapamycin or NVP-BEZ235, the intra- and extracellular TG concentrations, the lipid content and the protein content of FAS and ACCα were all lower than in the glucose-only groups. In addition, after co-treatment with glucose and the three inhibitors, the protein content of CPT1 was higher than that in the glucose-only treatment. Meanwhile, the extracellular VLDL concentration was higher after co-treatment with glucose and LY294002 or rapamycin, but it showed no evident change after co-treatment with glucose and NVP-BEZ235. The result of Western blotting (Fig. 3f) showed that 35 mmol/L glucose increased ACCα protein expression. After treatment with glucose and LY294002, rapamycin or NVP-BEZ235, ACCα protein expression was lower than in the 35-mmol/L glucose group. As can be seen in Fig. 4, Oil Red O staining revealed that 5 mmol/L and 35 mmol/L glucose caused an increase in lipid accumulation. After co-treatment with glucose and LY294002, rapamycin or NVP-BEZ235, lipid accumulation decreased. These results indicated that glucose regulates the lipid accumulation mediated by the PI3K-Akt-mTOR signaling pathway.

How many lipid metabolism pathways are involved in the regulation of lipid deposition mediated by the PI3K-Akt-mTOR signaling pathway? The mRNA expression levels of genes involved in lipogenesis, fatty oxidation and VLDL-TG assembly and secretion were measured. As shown in Figs. 5a-c, 5 mmol/L glucose increased the mRNA expression levels of genes involved

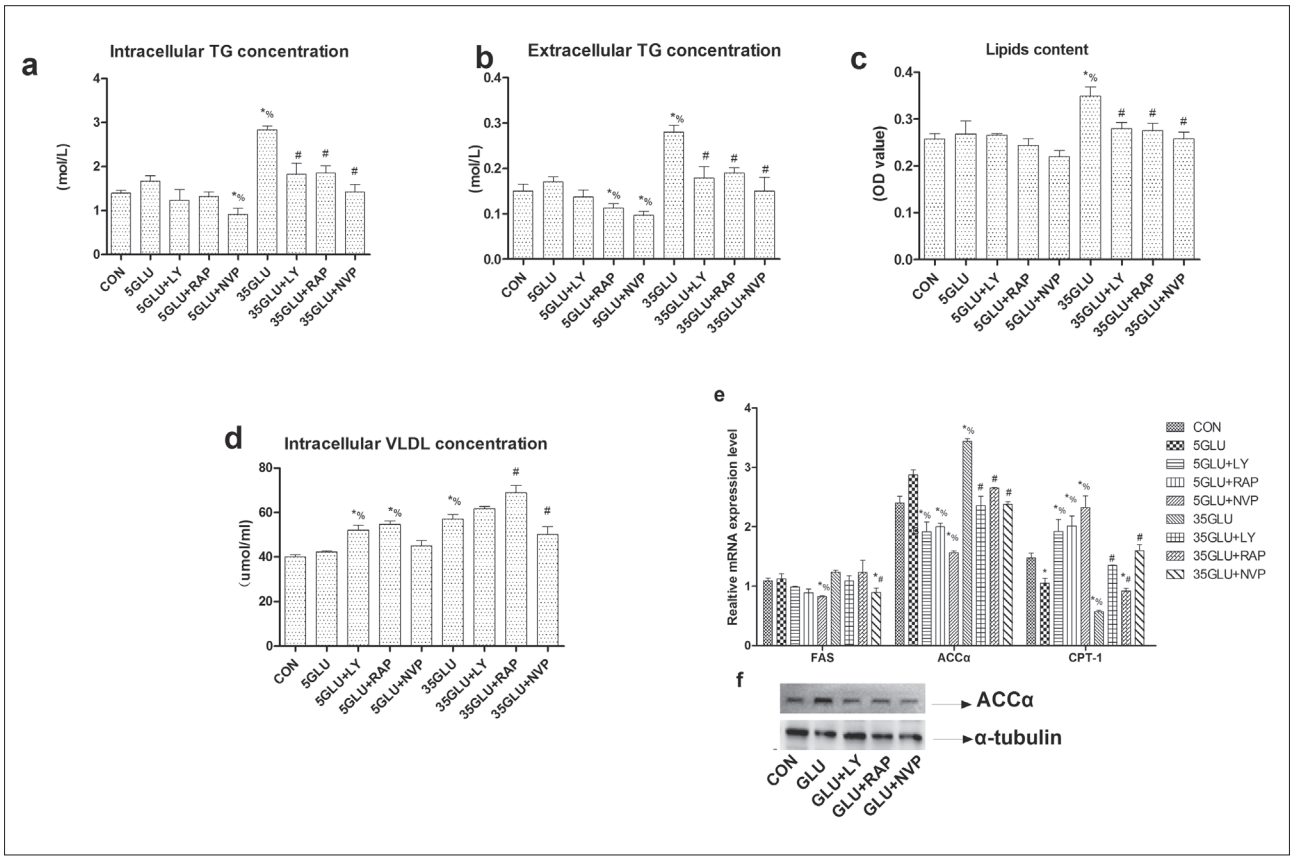

Fig. 3. Treatment with LY294002, rapamycin or NVP-BEZ235 changed the effect of glucose on lipid accumulation. **a** – intracellular TG concentration (mmol/L); **b** – extracellular TG concentration, (mmol/L); **c** – lipid content measured by Oil Red O extraction (optical density value); **d** – extracellular VLDL concentration (mg/ml); e – protein contents of genes involved in lipid metabolism: FAS (nmol/ml), ACCα and CPT1 (ng/ml); **f** – result of Western blotting for ACCα. The symbols "CON, 5GLU, 35GLU, LY, RAP, NVP" in the right legend and under the blot indicate control, 5 mmol/L glucose, 35 mmol/L glucose, 20 μmol/L LY294002, 30 nmol/L rapamycin, and 1 μmol/L NVP-BEZ235, respectively. "*" above the bars indicates significant differences between all groups and the control group at P<0.05; "%" above the bars indicates significant differences between all groups and 5GLU at P<0.05; "#" above the bars indicates significant differences between all groups and 35GLU at P<0.05.

in lipogenesis (sterol regulatory element-binding proteins (SREBPs), FAS, ACCα, carbohydrate response element binding protein (ChREBP) and liver X receptor α (LXRα)), while it decreased the mRNA expression levels of genes involved in fatty acid oxidation (peroxisome proliferator activated receptor α (PPARα), PPARγ, carnitine palmitoyltransferase 1 (CPT1) and acyl-CoA oxidase 1, palmitoyl (ACOX1)), and increased the mRNA expression levels of genes involved in VLDL-TG assembly and secretion (forkhead box O1 (FoxO1), microsomal triglyceride transfer protein (MTTP), and Apolipoprotein B (ApoB)). The mRNA expression levels of the detected genes in the 35-mmol/L glucose group were higher than those in the 5-mmol/L glucose group.

Compared with the mRNA expression levels of genes in the glucose group, after co-treatment with glucose and LY294002, rapamycin or NVP-BEZ235, the mRNA expression levels of the genes involved in lipogenesis (SREBP1, FAS, ACCα, ChREBP, and LXRα) decreased, the mRNA expression levels of the genes involved in fatty acid oxidation (PPARα, PPARγ, CPT1, and ACOX1) increased, and the mRNA expression levels of the genes involved in the VLDL-TG assembly and secretion (FoxO1, MTTP, and ApoB) also increased.

DISCUSSION

When abundant carbohydrate is available, glucose is converted to glycogen and fat, storage products that are used during fasting and strenuous exercise. Our previous results indicated that overfeeding could in-

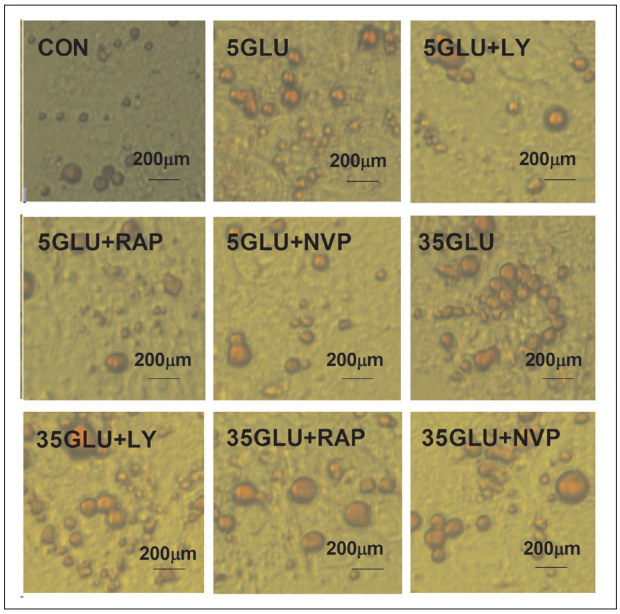

Fig. 4. Intracellular lipid accumulation measured by Oil Red O staining. The cells were examined by phase contrast microscopy at 200x magnification. The symbols "CON, 5GLU, 35GLU, LY, RAP, NVP" on the left side of each picture indicate control, 5 mmol/L glucose, 35 mmol/L glucose, 20 μmol/L LY294002, 30 nmol/L rapamycin, and 1 μmol/L NVP-BEZ235, respectively.

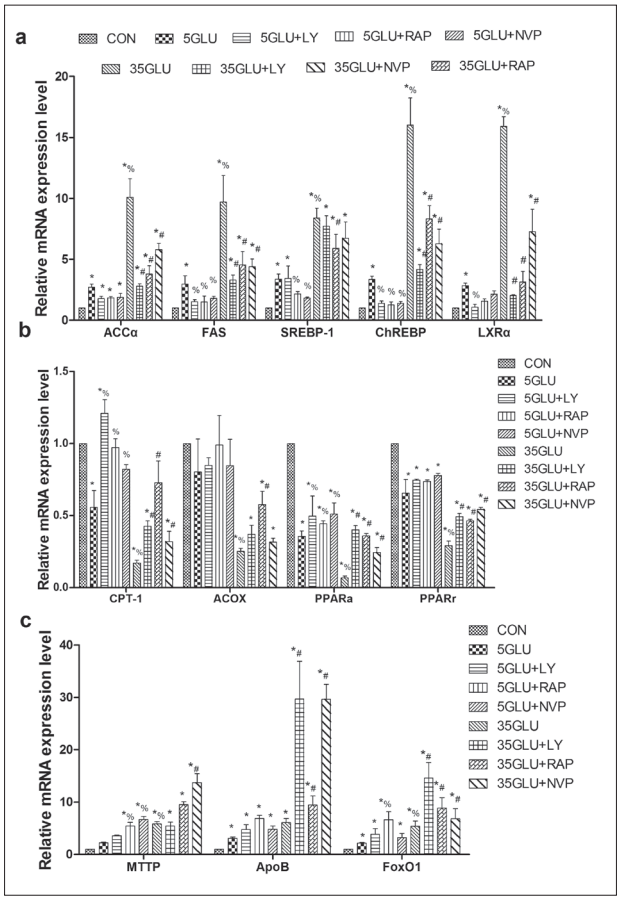

Fig. 5. Treatment with LY294002, rapamycin or NVP-BEZ235 changed the effect of glucose on lipid metabolism. **a** – relative mRNA expression levels of genes related to lipogenesis; **b** – relative mRNA expression levels of genes related to fatty acid oxidation; **c** – relative mRNA expression levels of genes related to VLDL-TG assembly and secretion. The symbols "CON, 5GLU, 35GLU, LY, RAP, NVP" in the right legend and under the blot indicate control, 5 mmol/L glucose, 35 mmol/L glucose, 20 μmol/L LY294002, 30 nmol/L rapamycin, and 1 μmol/L NVP-BEZ235, respectively. "*" above the bars indicates significant differences between all groups and the control group at P<0.05; "%" above the bars indicates significant differences between all groups and 5GLU at P<0.05; "#" above the bars indicates significant differences between all groups and 35GLU at P<0.05.

crease goose plasma insulin and glucose levels [10], and that insulin treatment could stimulate lipid deposition in goose primary hepatocytes via the PI3K-Akt-mTOR signaling pathway [8]. In this study, glucose was shown to stimulate lipogenesis, decrease fatty oxidation and increase VLDL assembly and secretion. Glucose increased the lipid deposition in goose primary hepatocytes, which was mediated by the PI3K-Akt-mTOR signaling pathway. The stimulation of lipogenesis and the inhibition of fatty acid oxidation by glucose favor hepatic lipid accumulation; however, the stimulation of VLDL-TG assembly and secretion limits lipid accumulation in liver cells.

The activated PI3K-Akt pathway has been linked to the development of hepatic steatosis [9]. It was previously shown that the Akt-mTOR signal transduction pathway is involved in lipid deposition in renal tubular cells in diabetes mellitus [17], and that the PI3K-Akt pathway is involved in the high glucose-induced increase of SREBP-1 in HKC [5]. However, the role of the PI3K-Akt-mTOR signaling pathway in glucose-induced lipid deposition has not been fully elucidated. We hypothesized that glucose induces lipid deposition in liver cells through the PI3K-Akt-mTOR signaling pathway. In this study, we first explored whether glucose affected the PI3K-Akt-mTOR pathway in goose liver cells. Similar to previous studies that revealed that high glucose affected the PI3K/Akt pathway in renal mesangial cells [18], human endothelial cells [19] and mouse cardiac fibroblasts [20], our results showed that the levels of total S6K (both phosphorylated and nonphosphorylated forms) increased after glucose treatment. The gene expression of related factors changed after the glucose treatment; thus it was

concluded that glucose could stimulate the PI3K-Akt-mTOR pathway.

The other aim was to investigate the role of the PI3K-Akt-mTOR pathway in glucose-induced lipid deposition. To that end, cells were treated with glucose and the PI3K inhibitor LY294002, mTOR inhibitor rapamycin, or PI3K and mTOR dual inhibitor NVP-BEZ235. Our results indicated that LY294002, rapamycin or NVP-BEZ235 all markedly inhibited the PI3K-Akt-mTOR signal pathway activation induced by glucose. Upregulation of lipogenesis was attenuated by the addition of LY294002, rapamycin or NVP-BEZ235 in cells under a glucose medium. Similarly, other researchers found that the PI3K-Akt pathway plays a role in glucose-mediated cellular lipid synthesis. Two recent reports showed that high fat diet (HFD)-induced hepatic steatosis was virtually eliminated in liver-specific PI3K p110-a$^{-/-}$ mice [21], and that the inhibition of hepatic Akt2 in mice ameliorates liver steatosis caused by a HFD [22], suggesting that PI3K-Akt can promote hepatic lipid accumulation under conditions of high dietary fat. Therefore, these results strongly support the fact that the PI3K-Akt-mTOR signaling pathway mediates glucose-induced lipid accumulation by upregulating fatty acid synthesis.

Whether lipid metabolism is similarly regulated in cells undergoing a glucose-induced proliferative response has not been investigated. Our results show that glucose can decrease the mRNA expression and protein contents of the products of genes involved in fatty acid oxidation and VLDL assembly and secretion; however, inhibition of PI3K-Akt-mTOR signaling abolishes the glucose-induced decrease in fatty acid oxidation and VLDL-TG assembly and secretion. Some studies revealed that increased mTOR activity impaired hepatocytic lipid homeostasis by regulating the transcription factors PPARα, PPARγ and retinoid X receptor b [23]. PI3K-Akt signaling executes many of the anabolic activities of growth factor-stimulated cells, including lipid and protein synthesis. Its involvement in suppressing glucose-induced fatty acid oxidation and VLDL-TG assembly and secretion at the cellular level is still unclear. When stimulated to proliferate, liver cells commit to net lipid synthesis by suppressing fatty acid oxidation and VLDL-TG assembly and secretion, concomitantly inducing lipid synthesis. The ability to suppress fatty acid oxidation and VLDL-TG assembly and secretion is required for these cells to achieve maximal rates of proliferation. These results identify a novel mechanism used to modulate lipid metabolism in proliferating cells. However, further studies are needed to determine the exact mechanism involved in PI3K-Akt-mTOR-mediated lipid deposition in proliferating liver cells.

In conclusion, our data describe the glucose-promoted stimulation of lipid deposition through the PI3K-Akt-mTOR-dependent pathway in goose primary hepatocytes.

Acknowledgments: This work was supported by the National Natural Science Funds of China Nos. 31101712 and 31672413.

Authors' contribution: CH and SW conceived and designed the experiments. The contribution of CH and SW is equal. QS, XX, DL and HW performed the experiments. HL and LL analyzed the data. HX and FX contributed to the reagents/materials. FY and XZ wrote the paper.

Conflict of interest disclosure: The authors declare that there is no conflict of interest.

REFERENCES

1. Jun H, Song Z, Chen W, Zanhua R, Yonghong S, Shuxia L, Huijun D. In vivo and in vitro effects of SREBP-1 on diabetic renal tubular lipid accumulation and RNAi-mediated gene silencing study. Histochem Cell Biol. 2009;131:327-45.
2. Morral N, Edenberg HJ, Witting SR, Altomonte J, Chu T, Brown M. Effects of glucose metabolism on the regulation of genes of fatty acid synthesis and triglyceride secretion in the liver. J Lipid Res. 2007;48:1499-510.
3. Saudemont A, Colucci F. PI3K signaling in lymphocyte migration. Cell Cycle. 2009;8:3307-10.
4. Engelman JA, Luo J, Cantley LC. The evolution of phosphatidylinositol 3-kinases as regulators of growth and metabolism. Nat Rev Genet. 2006;7:606-19.
5. Hao J, Liu S, Zhao S, Liu Q, Lv X, Chen H, Niu Y, Duan H. PI3K/Akt pathway mediates high glucose-induced lipogenesis and extracellular matrix accumulation in HKC cells through regulation of SREBP-1 and TGF-beta1. Histochem Cell Biol. 2011;135:173-81.
6. Ingram AJ, Ly H, Thai K, Kang MJ, Scholey JW. Mesangial cell signaling cascades in response to mechanical strain and glucose. Kidney Int. 1999;56:1721-8.
7. Heljic M, Brazil DP. Protein kinase B/Akt regulation in diabetic kidney disease. Front Biosci (Schol Ed). 2011;3:98-104.
8. Han C, Wei S, He F, Liu D, Wan H, Liu H, Li L, Xu H, Du X, Xu F. The regulation of lipid deposition by insulin in goose liver cells is mediated by the PI3K-Akt-mTOR signaling pathway. PLoS One. 2015;10:e98759.

9. Jackel-Cram C, Qiao L, Xiang Z, Brownlie R, Zhou Y, Babiuk L, Liu Q. Hepatitis C virus genotype-3a core protein enhances sterol regulatory element-binding protein-1 activity through the phosphoinositide 3-kinase-Akt-2 pathway. J Gen Virol. 2010;91:1388-95.
10. Han C, Wang J, Xu H, Li L, Ye J, Jiang L, Zhuo W. Effect of overfeeding on plasma parameters and mRNA expression of genes associated with hepatic lipogenesis in geese. Asian Austral J Anim. 2008;21:590-5.
11. Han C, Ye F, Shen X, Liu D, He F, Wei S, Xu H, Li L, Liu H. Change of the mTOR pathway in tissues of overfed geese. Revista Brasileira De Ciência Avícola. 2015;17:293-9.
12. Seglen PO. Preparation of isolated rat liver cells. Methods Cell Biol. 1976;13:29-83.
13. Fossati P, Prencipe L. Serum triglycerides determined colorimetrically with an enzyme that produces hydrogen peroxide. Clin Chem. 1982;28:2077-80.
14. Mori M, Itabe H, Higashi Y, Fujimoto Y, Shiomi M, Yoshizumi M, Ouchi Y, Takano T. Foam cell formation containing lipid droplets enriched with free cholesterol by hyperlipidemic serum. J Lipid Res. 2001;42:1771-81.
15. Ramirez-Zacarias JL, Castro-Munozledo F, Kuri-Harcuch W. Quantitation of adipose conversion and triglycerides by staining intracytoplasmic lipids with Oil Red O. Histochemistry. 1992;97:493-7.
16. Livak KJ, Schmittgen TD. Analysis of relative gene expression data using real-time quantitative PCR and the 2(-Delta Delta C(T)) Method. Methods. 2001;25:402-8.
17. Hao J, Zhu L, Li F, Liu Q, Zhao X, Liu S, Xing L, Feng X, Duan H. Phospho-mTOR: a novel target in regulation of renal lipid metabolism abnormality of diabetes. Exp Cell Res. 2013;319:2296-306.
18. Wu D, Peng F, Zhang B, Ingram AJ, Kelly DJ, Gilbert RE, Gao B, Kumar S, Krepinsky JC. EGFR-PLCgamma1 signaling mediates high glucose-induced PKCbeta1-Akt activation and collagen I upregulation in mesangial cells. Am J Physiol Renal Physiol. 2009;297:F822-F834.
19. Sheu ML, Ho FM, Yang RS, Chao KF, Lin WW, Lin-Shiau SY, Liu SH. High glucose induces human endothelial cell apoptosis through a phosphoinositide 3-kinase-regulated cyclooxygenase-2 pathway. Arterioscler Thromb Vasc Biol. 2005;25:539-45.
20. Venkatachalam K, Mummidi S, Cortez DM, Prabhu SD, Valente AJ, Chandrasekar B. Resveratrol inhibits high glucose-induced PI3K/Akt/ERK-dependent interleukin-17 expression in primary mouse cardiac fibroblasts. Am J Physiol Heart Circ Physiol. 2008;294:H2078-H2087.
21. Chattopadhyay M, Selinger ES, Ballou LM, Lin RZ. Ablation of PI3K p110-alpha prevents high-fat diet-induced liver steatosis. Diabetes. 2011;60:1483-92.
22. Leavens KF, Easton RM, Shulman GI, Previs SF, Birnbaum MJ. Akt2 is required for hepatic lipid accumulation in models of insulin resistance. Cell Metab. 2009;10:405-18.
23. Parent R, Kolippakkam D, Booth G, Beretta L. Mammalian target of rapamycin activation impairs hepatocytic differentiation and targets genes moderating lipid homeostasis and hepatocellular growth. Cancer Res. 2007;67:4337-45.